



# Plato's Error and a Mean Field Formula for Convex Mosaics

Gábor Domokos<sup>1</sup> · Zsolt Lángi<sup>2</sup>

Received: 12 July 2019 / Accepted: 2 August 2019  
© The Author(s) 2019

## Abstract

Plato claimed that the regular solids are the building blocks of all matter. His views, commonly referred to as the geometric atomistic model, had enormous impact on human thought despite the fact that four of the five Platonic solids can not fill space without gaps. In this paper we quantify these gaps, showing that the errors in Plato's estimates were quite small. We also develop a mean field approximation to convex honeycombs using a generalized version of Plato's idea. This approximation not only admits to view convex mosaics in  $d = 3$  dimensions as a continuum but we also find that it is quite accurate, showing that Plato's geometric intuition may have been remarkable.

**Keywords** Convex mosaic · Uniform mosaic · Platonic solid

**Mathematics Subject Classification** 52C22 · 52B11 · 52A38

## 1 Introduction

### 1.1 Plato's Idea

One of the greatest triumphs of Greek mathematics is undoubtedly the identification of the five regular solids. The time of discovery of the individual solids is very hard to trace, cubic dice were carved in Mesopotamia many thousand years ago and several dodecahedra of Etruscan and Celtic origin have been identified (Heath 1921). In

---

✉ Gábor Domokos  
domokos@iit.bme.hu

Zsolt Lángi  
zlangi@math.bme.hu

<sup>1</sup> MTA-BME Morphodynamics Research Group and Department of Mechanics, Materials and Structures, Budapest University of Technology, Műegyetem rakpart 1-3., Budapest 1111, Hungary

<sup>2</sup> MTA-BME Morphodynamics Research Group and Department of Geometry, Budapest University of Technology, Egy József utca 1., Budapest 1111, Hungary

fact, there is evidence (Atiyah and Sutcliffe 2003) that all five solids may have been known to the Neolithic people of Scotland around 2000BC, as demonstrated by the stone models which date from this period and are kept in the Ashmolean Museum in Oxford (1927.2727-31). Nevertheless, the unification of these concepts and the recognition of the significance of regular solids is mostly attributed to the Pythagoreans and to Theaetetus of Athens (Heath 1921), a pupil of Plato. The last (XIIIth) book of Euclid's *Elements* is dedicated to the study of the regular solids and it culminates by delivering an (albeit incomplete) proof that there exist exactly five such objects. Apparently, Plato recognized the great significance of the regular solids (Senechal 1981) (which now carry his name) and coupled this seminal geometric discovery with another fundamental idea of Greek (and in fact, Oriental) philosophy (Ball 2004): the four *elements*: earth, air, fire and water. The numbers (five solids versus four elements) were almost matched and he resolved this by assigning the fifth solid (the dodecahedron) as the building block of the cosmos. While Aristotle did not share Plato's views (on which we will elaborate later), it is remarkable that he also complemented the list of four elements with a fifth one (aether) (Lloyd 1968).

While it is beyond the scope of the current paper to present any novelty on the philosophical interpretation of Plato's *Timaeus* (Plato 2015), given the broad range of existing interpretations of this text (Wilberding and Horn 2012) it might be appropriate to indicate which is closest to our current approach. In this respect the work of Whitehead (1938) is certainly relevant as we regard Plato's interpretation of the *Elements* as static ideal forms. We mention that dynamic interpretations, in the context of the perpetually incomplete Universe, also exist (Zeyl and Sattler 2019). Plato regards (Plato 2015) the Universe as the purposeful work of the divine Craftsman (Demiurge) (Perl 1998) and the *Elements* (and their realization as the regular solids) can be viewed as part of the activity of the Demiurge who created these regular geometric shapes. It is a highly interesting subject how the regular solids reflect the perceived qualities (Albertazzi 2013) of the *Elements* and how the latter are related to our contemporary thinking about our environment (Macauley 2010) however, we will not explore these avenues in this paper.

Plato's theory, representing a distinct direction of classical Greek philosophy, is commonly referred to as the *geometric atomistic model* (Wilberding and Horn 2012) and it had enormous impact on human thought.

Despite its philosophical significance, Plato's atomistic theory is, from the point of view of theoretical physics, at first sight, merely a 'beautiful mistake' (Wilczek 2011). Nevertheless, at closer inspection, one discovers the seeds of modern atomic theory: reducing the physical world to a few indivisible substances existing in great numbers of identical copies coincides with our current understanding. Also, Nobel laureate Wilczek (2011) hails Plato's insight that symmetry defines structure as particularly deep. So, from the physical point of view, Plato's theory appears to be *technically flawed*, nevertheless, it contains deep ideas, inspiring even for modern science.

Since Plato's ideas appear to be deeply rooted in geometric intuition, it might be appropriate to take a close look at his model by using the tools of modern convex geometry. Our goal is to show that, analogously to the physics approach, we find *technical flaws*, however, there are deep ideas and in this paper we make an attempt

to carry these ideas somewhat further. While Plato did not claim (Plato 2015) explicitly that regular solids fill space *without gaps*, his critics, foremost Aristotle (Senchal 1981) pointed out that this would be a logical consequence of his theory. Apparently, Plato's claim, or at least its logical consequence, appears to contain some kind of geometric error, except in the case of the cube. In order to quantify this error we will use the concept of solid angles, certainly not available to the Greeks. Despite this fact, as we will show, the quantitative errors (which we may call the technical flaws of Plato's geometric theory) appear to be rather small. Since Plato's main interest was philosophy rather than geometry, we will attempt to give another interpretation to his model which ignores small mismatches and can be generalized to an approximation which we call a mean field theory. The natural framework to study the geometry of space-filling by polyhedra is the geometric theory of convex mosaics the basic concepts of which we outline below and then we apply these tools to interpret and generalize Plato's ideas.

## 1.2 Definition and Brief History of Mosaics

A  $d$ -dimensional *mosaic*  $\mathcal{M}$  is a countable system of compact domains in  $\mathbb{R}^d$ , with nonempty interiors, that cover the whole space and have pairwise no common interior points (Schneider and Weil 2008). We call a mosaic *convex* if these domains are convex and in this case all domains are convex polytopes (Schneider and Weil 2008, Lemma 10.1.1). In this paper we deal only with convex mosaics. We call these polytopes the *cells* of the mosaic, and the faces, edges and vertices of the cells the *faces*, *edges* and *nodes* of the mosaic, respectively. A cell having  $v$  vertices is called a *cell of degree*  $v$ , and a node which is the vertex of  $n$  cells is called a *node of degree*  $n$ . Our prime focus is to determine how average values of these quantities, denoted by  $\bar{n}$  and  $\bar{v}$ , respectively, depend on each other. We remark that for planar regular mosaics, the pair  $\{\bar{v}, \bar{n}\}$  is called the Schläfli symbol of the mosaic so, by generalizing this concept, we will refer to the  $[\bar{n}, \bar{v}]$  plane as the *symbolic plane* of convex mosaics. These, and closely related global averages have been studied before and proved to be powerful tools in the geometric study of mosaics: in Chung et al. (2012) the planar isoperimetric problem restricted to convex polygons with  $v < 6$  vertices is resolved using these quantities.

Our main focus will be *face-to-face* mosaics, in which each face of the mosaic (that is, each face of any cell of the mosaic) is the face of exactly two cells. Unless stated otherwise, any mosaic discussed in our paper will be a convex face-to-face mosaic. Furthermore, we assume that the mosaic is *normal*, that is, for some  $0 < r < R$  each cell contains a ball of radius  $r$ , and is contained in a ball of radius  $R$  (see, e.g. Schulte 1993). This implies, in particular, that the volumes of the cells are bounded from above, and that the mosaic is *locally finite*; that is, each point of space belongs to finitely many cells. We note that a precise definition of  $\bar{v}$  and  $\bar{n}$  can be obtained in the usual way, that is, by taking the limit of the average degrees of cells/nodes contained in a large ball whose radius tends to infinity. Here, we always tacitly assume that these limits exist.

Geometric intuition suggests that  $\bar{v}$  and  $\bar{n}$  should have an inverse-type relationship: more polytopes meeting at a node implies smaller internal angles in the polytopes, which, in turn, suggests a smaller number of vertices for each polytope. One can (Domokos and Lángi 2019) in fact, express the nodal degree  $\bar{n}$  also by the average internal angle  $\bar{\Omega}$  as

$$\bar{n} = \frac{S_{d-1}}{\bar{\Omega}} \quad (1)$$

where  $S_{d-1}$  denotes the surface area of the  $(d-1)$ -dimensional ball, i.e. the total angle in  $d$ -dimensions. In one dimension ( $d=1$ ) we have  $v=n=2$  for each cell and vertex. In two dimensions one can have cells and nodes of various degrees, nonetheless, it is known (Schneider and Weil 2008, Theorem 10.1.6) that for all convex mosaics

$$\bar{n} = 2\bar{v}/(\bar{v}-2), \quad (2)$$

thus convex mosaics in  $d=2$  dimensions are represented by a 1-dimensional continuum on the  $[\bar{n}, \bar{v}]$  symbolic plane.

The situation in  $d=3$  dimensions appears, at least at first sight, to be radically different. (Schneider and Weil 2008) provide the general equations governing 3D random mosaics showing that, beyond the trivial inequalities  $\bar{n}, \bar{v} \geq 4$  these formulae do not yield additional constraints on  $\bar{n}, \bar{v}$  suggesting that in the  $[\bar{n}, \bar{v}]$  symbolic plane, except for the unphysical domains characterized by  $\bar{n}, \bar{v} < 4$ , we might expect to see mosaics *anywhere*. However, this is not the case if we look at the best known mosaics: uniform honeycombs. The latter are a special class of convex mosaics where cells are congruent, uniform polyhedra and all nodes are identical under translation. The list of all possible convex uniform honeycombs was completed only recently by Johnson (1991) who described 28 such mosaics (for more details on the 28 uniform honeycombs see Grünbaum 1994; Deza and Shtogrin 2000 and more details on the history see Senechal 1981). To provide the complete list of these 28 honeycombs has been a major result in discrete geometry. On the  $[\bar{n}, \bar{v}]$  symbolic plane the points corresponding to these mosaics appear to accumulate on a narrow stripe (cf. Fig. 1, Table 2) which may suggest that, in some way analogous to the 2D case, there exists a continuum representing 3D mosaics on the symbolic plane. However, by studying the data in Table 2 we can see that there can not even exist any *exact* formula of the type

$$\bar{n} = F(\bar{f}, \bar{v}) \quad (3)$$

analogous to (2), since, for example, the dual of the cantellated cubic honeycomb (4') is characterized by  $(\bar{n}, \bar{f}, \bar{v}) = (12, 5, 6)$  and the dual of the runcic cubic honeycomb (9') is characterized by  $(\bar{n}, \bar{f}, \bar{v}) = (10, 5, 6)$ . Our goal is to offer some partial understanding of this phenomenon by introducing, based on Plato's ideas, a mean field approximation of type (3). To explain this approach we first analyze Plato's original claims.

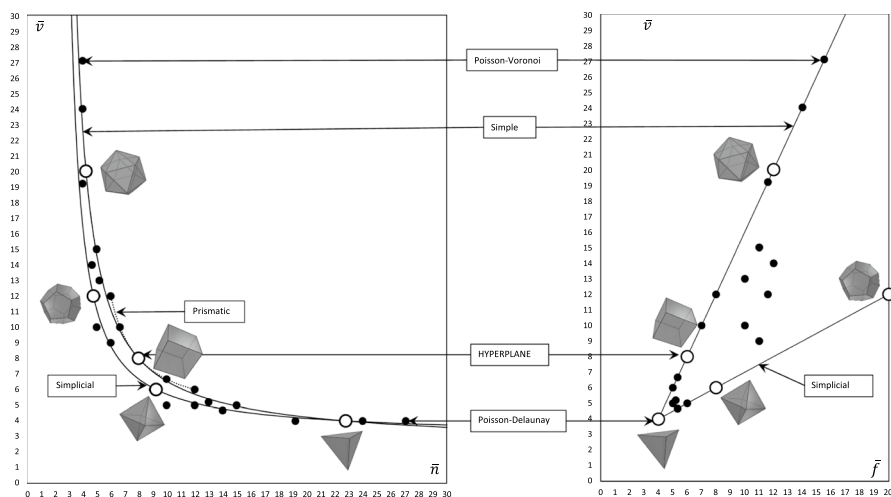


**Fig. 1** The 28 uniform honeycombs, their duals, the hyperplane mosaics, the Poisson-Voronoi and Poisson-Delaunay mosaics shown as black dots on the symbolic plane  $[\tilde{n}, \tilde{v}]$  (left) and on the plane  $[\tilde{f}, \tilde{v}]$  (right). Mosaics (virtual or real) associated with the five Platonic solids shown as circles in both diagrams (for numerical data associated with the 5 Platonic solids see Table 1). Continuous straight lines on the right panel correspond to simple and simplicial polyhedra. Dotted line on the left panel corresponds to prismatic mosaics. Continuous curves on the left panel show the Platonic approximation associated with the latter. For detailed numerical data see Table 2

### 1.3 Interpretation of Plato's Error

Plato's idea was resurrected in the study of non-Euclidean mosaics (Coxeter 1956) where, by choosing suitable sign for the curvature, all Platonic solids fill space without gaps so, in this broader setting, there is no error at all. Our main target is nevertheless Euclidean space which imposes strict constraints on the geometry of mosaics and our goal is to explain how, under these constraints, some part of the Platonic idea may be salvaged and also serve the understanding of Euclidean mosaics.

Using the framework of convex mosaics and the concept of the symbolic plane, Plato's error can be interpreted in several ways. Apparently, except for the cube, it is not possible to obtain the total solid angle  $S_2 = 4\pi$  at one node by assembling an *integer* number of any of the other four Platonic solids. In other words, we may say that Eq. (1) can not be fulfilled if  $\tilde{n}$  is an integer. However, since our (hypothetical) mosaic contains only one type of cell,  $\tilde{n}$  has to be an integer. As a consequence, we have to admit some error term either in the solid angle  $\tilde{\Omega}$  or in the nodal degree  $\tilde{n}$ ; essentially it is the same error expressed in two different ways. If we substitute the exact value of  $\Omega(f, v)$  associated with the Platonic solid with  $f$  faces and  $v$  vertices into Eq. (1) then we obtain a *virtual nodal degree*  $\hat{n}$  as

$$\hat{n}(f, v) = \frac{4\pi}{\Omega(f, v)} \quad (4)$$

**Table 1** Regular polyhedra, their solid angles and Plato's error  $E_0$  [shown in Eq. (5)] expressing the solid angle mismatch at the nodes

ID.	Name	$f$	$v$	$\Omega$	$\hat{n} = 4\pi/\Omega$	$[\hat{n}]$	$e_1(\%)$
1	Tetrahedron	4	4	0.551	22.79	23	0.9
2	Cube	6	8	1.571	8.00	8	0.0
3	Octahedron	8	6	1.359	9.24	9	2.7
4	Dodecahedron	12	20	2.635	4.77	5	4.6
5	Icosahedron	20	12	2.962	4.24	4	6.1

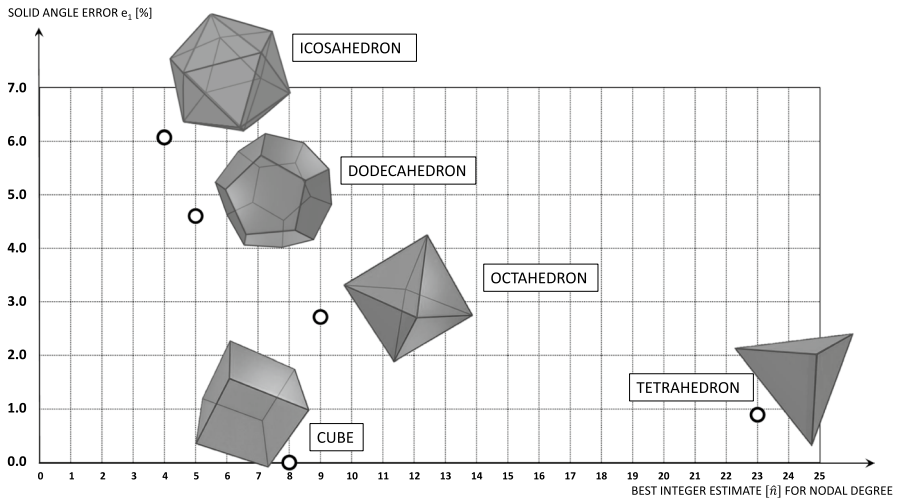


**Fig. 2** The five regular solids interpreted as cells of a convex honeycomb. Horizontal axis shows the best (integer) approximation for the nodal degree  $\hat{n}$ , vertical axis shows the relative error  $E_0 = \left| 1 - \frac{\hat{n}}{[\hat{n}]} \right|$ , indicating the mismatch in the solid angle (absolute value of angular excess or deficit) at such an imaginary node. We can observe that only the cube can be used as a cell of a honeycomb, nonetheless, the relative errors are rather small also in case of the other 4 regular solids

associated with the Platonic solid with  $f$  faces and  $v$  vertices. The error may be expressed as

$$E_0 = \left| 1 - \frac{\hat{n}}{[\hat{n}]} \right|, \quad (5)$$

where  $[\cdot]$  denotes rounding to the nearest integer. This is illustrated in Fig. 2, numerical data is summarized in Table 1. We may observe that the errors are remarkably small ( $< 10\%$ ) for all Platonic solids.

Observe that (4) is reminiscent of the elusive formula (3), albeit, it is interpreted only for pairs  $(f, v)$  associated with the 5 Platonic solids. Our goal is to carry this idea further and expand it into a mean field model encompassing all convex mosaics.

**Table 2** Uniform convex honeycombs, their duals, Poisson-Voronoi, Poisson-Delaunay and Hyperplane random mosaics, and the approximation error  $E$  [given in Eq. (7)] by Platonic mosaics

ID.	Name of mosaic	$\bar{n}$	$\bar{v}$	$\bar{f}$	$\hat{n}$	$E(\%)$
1	Cubic	8	8	6	8.00	0.0
2	Rectified cubic	6	9	11	6.13	2.2
3	Truncated cubic	5	15	11	4.75	4.9
4	Cantellated cubic	5	12	11.6	5.16	3.3
5	Cantitruncated cubic	4	$19\frac{1}{5}$	$11\frac{3}{5}$	4.33	8.2
6	Runcitruncated cubic	5	15	11	4.75	4.9
7	Alternated cubic	14	$4\frac{2}{3}$	$5\frac{1}{3}$	14.66	4.7
8	Cantic cubic	5	15	11	4.75	4.9
9	Runcic cubic	5	10	10	5.87	17.3
10	Runcicantic cubic	4	24	14	3.91	2.2
11	Bitruncated cubic	4	24	14	3.91	2.2
12	Omnitruncated cubic	4	24	14	3.91	2.2
13	Quarter cubic	8	8	6	8.00	0.0
14	Truncated/bitruncated square prismatic	6	12	8	5.70	5.1
15	Snub square prismatic	10	$6\frac{2}{3}$	$5\frac{1}{3}$	9.77	2.3
16	Triangular prismatic	12	6	5	11.17	6.9
17	Hexagonal prismatic	6	12	8	5.70	5.1
18	Trihexagonal prismatic	8	8	6	8.00	0.0
19	Truncated hexagonal prismatic	6	12	8	5.70	5.1
20	Rhombi-hexagonal prismatic	8	8	6	8.00	0.0
21	Snub-hexagonal prismatic	10	$6\frac{2}{3}$	$5\frac{1}{3}$	9.77	2.3
22	Truncated trihexagonal prismatic	6	12	8	5.70	5.1
23	Elongated triangular prismatic	10	$6\frac{2}{3}$	$5\frac{1}{3}$	9.77	2.3
24	Gyrated alternated cubic	14	$4\frac{2}{3}$	$5\frac{1}{3}$	14.66	4.7
25	Gyroelongated alternated cubic	13	$5\frac{1}{5}$	$5\frac{1}{5}$	12.81	1.5
26	Elongated alternated cubic	13	$5\frac{1}{5}$	$5\frac{1}{5}$	12.81	1.5
27	Gyrated triangular prismatic	12	6	5	11.17	6.9
28	Gyroelongated triangular prismatic	10	$6\frac{2}{3}$	$5\frac{1}{3}$	9.77	2.3
29	Poisson-Voronoi	4	27.07	15.51	3.73	6.7
30	Hyperplane	8	8	6	8.00	0.0
1'	Dual of cubic	8	8	6	8.00	0.0
2'	Dual of rectified cubic	9	6	8	9.24	2.7
3'	Dual of truncated cubic	15	5	5	13.76	8.3
4'	Dual of cantellated cubic	12	5	6	12.62	5.2
5'	Dual of cantitruncated cubic	$19\frac{1}{5}$	4	4	22.79	18.7
6'	Dual of runcitruncated cubic	15	5	5	13.76	8.3
7'	Dual of alternated cubic	$4\frac{2}{3}$	14	12	4.79	2.6
8'	Dual of cantic cubic	15	5	5	13.76	8.3
9'	Dual of runcic cubic	10	5	6	12.62	26.2
10'	Dual of runcicantic cubic	24	4	4	22.79	5.0

**Table 2** (continued)

ID.	Name of mosaic	$\bar{n}$	$\bar{v}$	$\bar{f}$	$\bar{h}$	$E(\%)$
11'	Dual of bitruncated cubic	24	4	4	22.79	5.0
12'	Dual of omnitruncated cubic	24	4	4	22.79	5.0
13'	Dual of quarter cubic	8	8	6	8.00	0.0
14'	Dual of truncated/bitruncated square prismatic	12	6	5	11.17	6.9
15'	Dual of snub square prismatic	$6\frac{2}{3}$	10	7	6.54	1.9
16'	Dual of triangular prismatic	6	12	8	5.70	5.1
17'	Dual of hexagonal prismatic	12	6	5	11.17	6.9
18'	Dual of trihexagonal prismatic	8	8	6	8.00	0.0
19'	Dual of truncated hexagonal prismatic	12	6	5	11.17	6.9
20'	Dual of rhombi-hexagonal prismatic	8	8	6	8.00	0.0
21'	Dual of snub-hexagonal prismatic	$6\frac{2}{3}$	10	7	6.54	1.9
22'	Dual of truncated trihexagonal prismatic	12	6	5	11.17	6.9
23'	Dual of elongated triangular prismatic	$6\frac{2}{3}$	10	7	6.54	1.9
24'	Dual of gyrated alternated cubic	$4\frac{2}{3}$	14	12	4.79	2.6
25'	Dual of gyroelongated alternated cubic	$5\frac{1}{5}$	13	10	5.15	0.9
26'	Dual of elongated alternated cubic	$5\frac{1}{5}$	13	10	5.15	0.9
27'	Dual of gyrated triangular prismatic	6	12	8	5.70	5.1
28'	Dual of gyroelongated triangular prismatic	$6\frac{2}{3}$	10	7	6.54	1.9
29'	Dual of Poisson-Voronoi: Poisson-Delaunay	27.07	4	4	22.79	15.8
30'	Dual of Hyperplane: Hyperplane	8	8	6	8.00	0.0

Average error is 6.6%, maximal error is 26.2 %

## 1.4 Platonic Approximation of Mosaics

Our goal is to extend the domain of formula (4) to arbitrary values  $(\bar{f}, \bar{v})$  and this construction we will call a (real or virtual) *Platonic mosaic* associated to geometric mosaics with averages  $(\bar{f}, \bar{v})$ .

A cell in a  $d$ -dimensional mosaic  $\mathcal{M}$  is characterized by  $d$  integers  $m_i$  ( $i = 0, 1, 2 \dots d - 1$ ) defining the numbers of  $i$ -dimensional faces. We will refer to these scalars as the *cell descriptors*.

**Remark 1** Our choice of cell descriptors is, of course, arbitrary. For example, we did not include overall descriptors such as elongation, isoperimetric ratio or the average of angles. Our choice was motivated by the mean field model we intend to construct.

In a random mosaic the cell descriptors associated with a *typical cell* (Schneider and Weil 2008) are  $d$  random variables corresponding the aforementioned scalars. Motivated by this we introduce



**Definition 1** The average cell of a  $d$ -dimensional mosaic  $\mathcal{M}$  is a geometric model using the  $d$  average values  $\bar{m}_i, i = 0, 1, \dots, d - 1$  of cell descriptors associated with  $\mathcal{M}$  as cell descriptors and the assumption that all angles between  $i$ -dimensional faces are equal. If the descriptors  $\bar{m}_i$  are identical to the descriptors of a  $d$ -dimensional regular polytope then we call the average cell *real*, otherwise we call it a *virtual cell*. We will refer to the (real or virtual) mosaic composed of the average cell as a *Platonic mosaic* associated with  $\mathcal{M}$  and we denote it by  $P(\mathcal{M})$ . We call a Platonic mosaic *real* if the average cell is real and it fills space without gaps.

We may regard the associated Platonic mosaic  $P(\mathcal{M})$  as a mean field approximation of  $\mathcal{M}$ .

**Remark 2** Let  $\mathcal{M}$  be a mosaic in 2D and let  $P(\mathcal{M})$  be its Platonic approximation. The average cell of  $\mathcal{M}$  will be real if and only if  $\bar{v}(\mathcal{M})$  is an integer and  $P(\mathcal{M})$  will be real if and only if  $\bar{v}(\mathcal{M}) \in \{3, 4, 6\}$ . This follows from the fact that the only regular polygons filling the Euclidean plane are the regular triangle, the square and the regular hexagon.

**Remark 3** Let  $\mathcal{M}$  be a mosaic in 3D and  $P(\mathcal{M})$  be its Platonic approximation. The average cell of  $\mathcal{M}$  will be real if and only if

$$(\bar{v}(\mathcal{M}), \bar{f}(\mathcal{M})) \in \{(4, 4), (6, 8), (8, 6), (12, 20), (20, 12)\}$$

and  $P(\mathcal{M})$  will be real if and only if  $(\bar{v}(\mathcal{M}), \bar{f}(\mathcal{M})) = (8, 6)$  and in this case  $P(\mathcal{M})$  will be the cubic grid. This follows from the fact that the only space-filling Platonic solid is the cube.

Our key observation is the following

**Remark 4** While virtual cells do not admit the global construction of a polytope, they might still admit the computation of vertex angles and nodal angles. We will denote all quantities computed based on the average cell by  $\hat{\cdot}$ . Using this concept we can determine the solid angle  $\hat{\Omega}$  at a vertex and instead of (4) we may write

$$\hat{n}(\bar{f}, \bar{v}) = \frac{4\pi}{\hat{\Omega}(\bar{f}, \bar{v})}, \quad (6)$$

with the error term:

$$E = \left| 1 - \frac{\hat{n}}{\bar{n}} \right|, \quad (7)$$

so we see that the concept of Platonic mosaics is a natural, straightforward extension of Plato's original idea.

Using this concept we immediately have a heuristic argument supporting formula (2) result for planar mosaics. To construct the average cell in  $d = 2$  dimensions we

just need the average number  $\bar{v}$  of vertices; for the angles we use the fact that they are constant in the average cell. Now we can construct the average cell as a polygon with  $\bar{v}$  vertices. If  $\bar{v}$  is an integer then the average cell is real because it can be realized as a regular polygon with internal angles  $\alpha = \pi(\bar{v} - 2)/\bar{v}$ . However, if  $\bar{v}$  is not an integer this formula still yields an angle. Next we construct a *virtual node* to compute the approximation  $\hat{n}$  for the nodal degree  $\bar{n}$  as  $\hat{n} = 2\pi/\alpha = 2\bar{v}/(\bar{v} - 2)$ . While this is certainly a heuristic argument, it *happens* to provide the exact formula for all convex mosaics in the plane.

We certainly do not expect this construction to be exact for all mosaics, nevertheless, the above examples suggest that it may serve as a useful approximation. In  $d = 3$  dimensions we have 2 independent integer-type cell descriptors: the number  $v$  of vertices and the number  $f$  of faces with averages  $\bar{v}, \bar{f}$  and the main result of our paper concerns this case:

**Theorem 1** *In  $d = 3$  dimensions, the average cell yields the following approximation  $\hat{n}$  for the nodal degree based on the cell descriptors  $\bar{v}, \bar{f}$ :*

$$\hat{n}(\bar{v}, \bar{f}) = \frac{2\pi\bar{v}}{2(\bar{v} + \bar{f} - 2) \arcsin\left(\frac{\cos\left(\frac{\bar{v}\pi}{2(\bar{v} + \bar{f} - 2)}\right)}{\cos\left(\frac{(\bar{v} - 2)\pi}{2(\bar{v} + \bar{f} - 2)}\right)}\right) - (\bar{f} - 2)\pi}. \quad (8)$$

Based on which we can formulate.

**Theorem 2** *In case of the 28 uniform honeycombs, their duals, hyperplane mosaics, Poisson-Voronoi mosaics and Poisson-Delaunay mosaics we have an average error  $E_{\text{average}} \leq 7\%$  and a maximal error  $E_{\text{max}} \leq 27\%$ .*

Beyond the relatively small quantitative errors, the formula in Theorem 1 has other remarkable features. This formula may be formally interpreted over all pairs  $(\bar{f}, \bar{v}) \in \mathbb{R}^2$ . However, we should keep in mind that these numbers represent averages for the numbers of faces and vertices of convex polyhedra. Steinitz proved (Steinitz 1906, 1922) that for any convex polyhedron the inequalities  $v \geq 4$ ,  $\frac{1}{2}v + 2 \leq f \leq 2v - 4$  hold. The extreme cases corresponding to

$$f = 2v - 4, \quad v = 2f - 4 \quad (9)$$

are called simplicial and simple polyhedra, respectively, and the only polyhedron in both categories is the tetrahedron with  $f = v = 4$ . Since these are extreme cases, we can see that they also provide the extremes for the averages  $\bar{f}, \bar{v}$ . The left panel of Fig. 2 shows these straight lines which indeed provide a hull for all convex mosaics. If we regard the values provided by (9) as averages  $\bar{f}, \bar{v}$ , and substitute these averages into the formula of Theorem 1, the latter yields two curves on the symbolic plane  $[\bar{n}, \bar{v}]$ . While these curves (shown with solid lines on the left panel) do not provide a *hull* for the illustrated 60 mosaics, the range between the curves appears to be a reasonable approximation of the actual observed range. This illustrates that Platonic approximations may capture some essential characteristics of 3D mosaics.

In the next section we prove Theorems 1 and 2, and in Sect. 3 we summarize our findings.

## 2 Proof of the Theorems

### 2.1 Proof of Theorem 1: The Construction of the Average Cell

In the proof we use the next lemma.

**Lemma 1** Let  $S$  be the tetrahedron with vertices  $a = \left(\cos \frac{\alpha}{2}, -\sin \frac{\alpha}{2}, 0\right)$ ,  $b = \left(\cos \frac{\alpha}{2}, \sin \frac{\alpha}{2}, 0\right)$ ,  $o = (0, 0, 0)$  and  $m = (0, 0, \mu)$ . For  $x \in \{a, b, o, m\}$ , let  $\Omega_x$  denote the solid angle of  $S$  at  $x$ . Then

$$\Omega_m = \alpha + 2 \arccos \frac{\mu \sin \frac{\alpha}{2}}{\sqrt{\mu^2 + \cos^2 \frac{\alpha}{2}}} - \pi, \quad \Omega_o = \alpha, \quad (10)$$

and

$$\Omega_a = \Omega_b = \arccos \frac{\mu \sin \frac{\alpha}{2}}{\sqrt{\mu^2 + \cos^2 \frac{\alpha}{2}}} + \arccos \frac{\cos \frac{\alpha}{2}}{\sqrt{\mu^2 + \cos^2 \frac{\alpha}{2}}} - \frac{\pi}{2}. \quad (11)$$

**Proof** Note that the solid angle of  $S$  at a vertex  $x$  is equal to the area of the radial projection of  $S$  onto the unit sphere  $x + S^2$  centered at  $x$ . This projection is a spherical triangle, the angles of which are equal to the dihedral angles of  $S$  between pairs of faces meeting at  $x$ . It is well known that the area of a spherical triangle, with angles  $\alpha, \beta, \gamma$ , is equal to the excess angle  $\alpha + \beta + \gamma - \pi$ . Thus, to prove Lemma 1, it is sufficient to compute the dihedral angles of  $S$ . In the following, if  $x, y$  are distinct vertices of  $S$ , we denote the dihedral angle of  $S$  at the edge  $xy$  by  $\angle_S(xy)$ .

Clearly,  $\angle_S(om) = \alpha$ ,  $\angle_S(oa) = \angle_S(ob) = \frac{\pi}{2}$ , implying  $\Omega_o = \alpha$ , and by symmetry,  $\angle_S(ma) = \angle_S(mb)$ . The cross-section of  $S$  with the  $[x, z]$  coordinate plane is a triangle  $T$  whose vertices are  $o, m$  and the midpoint  $u = \left(\cos \frac{\alpha}{2}, 0, 0\right)$  of  $ab$ . This triangle has a right angle at  $o$ , and its legs are of length  $\mu$  and  $\cos \frac{\alpha}{2}$ . Observe that  $\angle_S(ab)$  is the angle of  $T$  at  $u$ , and thus, it is equal to

$$\angle_S(ab) = \arccos \frac{\cos \frac{\alpha}{2}}{\sqrt{\mu^2 + \cos^2 \frac{\alpha}{2}}}.$$

The exterior unit normal vector of the face  $abm$  of  $S$  is

$$v_1 = \left( \frac{\mu}{\sqrt{\mu^2 + \cos^2 \frac{\alpha}{2}}}, 0, \frac{\cos \frac{\alpha}{2}}{\sqrt{\mu^2 + \cos^2 \frac{\alpha}{2}}} \right).$$

The interior unit normal vector of the face  $oam$  is  $v_2 = \left( \sin \frac{\alpha}{2}, \cos \frac{\alpha}{2}, 0 \right)$ . Since  $v_1$  is the rotated copy of  $v_2$  around the line of  $am$  with angle  $\angle_S(am)$ ,  $\angle_S(am)$  is the angle between  $v_1$  and  $v_2$ . The inner product of  $v_1$  and  $v_2$  is equal to  $\langle v_1, v_2 \rangle = \cos \angle_S(am)$ , and thus, we have:

$$\angle_S(am) = \angle_S(bm) = \arccos \frac{\mu \sin \frac{\alpha}{2}}{\sqrt{\mu^2 + \cos^2 \frac{\alpha}{2}}}.$$

Now the rest of the solid angles can be computed from the dihedral angles as

$$\Omega_m = \angle_S(am) + \angle_S(bm) + \angle_S(om) - \pi, \quad \Omega_a = \Omega_b = \angle_S(am) + \angle_S(ab) + \angle_S(ao) - \pi.$$

□

Now we prove Theorem 1.

**Proof of Theorem 1** An average cell in the mosaic has  $\bar{f}$  faces,  $\bar{v}$  vertices and  $\bar{e} = \bar{v} + \bar{f} - 2$  edges. In our model, we denote the number of cells meeting at a node by  $\hat{n} = \hat{n}(\bar{v}, \bar{f})$ . A face of an average cell has  $\bar{e}_f = \frac{2\bar{e}}{\bar{f}}$  edges, and, within the cell, the degree of a vertex is  $\bar{v}_c = \frac{2\bar{e}}{\bar{v}}$ .

Based on Definition 1, we imagine an average cell as a polyhedron with ‘regular’  $\bar{e}_f$ -gons as faces such that the projection of the center of the polyhedron onto the plane of a face coincides with the center of the face. Let us decompose such a cell into tetrahedra whose vertices are two vertices of an edge of the cell, the center of one of the two faces containing this edge, and the center of the cell. Note that in this way we decompose the cell into  $2\bar{e}$  congruent tetrahedra. Let  $S$  be such a tetrahedron, and let  $ab$  denote the edge,  $o$  the center of the face and  $m$  the center of the cell in  $S$ . Let  $\Omega_m$  denote the solid angle of  $S$  at  $m$ , and  $\Omega_a$  the solid angle of  $S$  at  $a$ . Note that since these tetrahedra are congruent,  $\Omega_m = \frac{4\pi}{2\bar{e}} = \frac{2\pi}{\bar{e}}$ , and the solid angle of the cell at  $a$  is  $2\bar{v}_c\Omega_a$ . This angle is equal to  $\frac{4\pi}{\hat{n}}$ , implying that  $\Omega_a = \frac{2\pi}{\bar{v}_c\hat{n}} = \frac{\pi\bar{v}}{\bar{e}\hat{n}}$ , from which

$$\hat{n} = \frac{\pi\bar{v}}{\bar{e}\Omega_a}. \quad (12)$$

Using Lemma 1, we compute  $\Omega_a$  as a function of  $\bar{e}$ ,  $\bar{v}$  and  $\bar{f}$ . In our computations, for simplicity, we use the notations of Lemma 1. Then we have  $\frac{\alpha}{2} = \frac{2\pi}{2\bar{e}_f} = \frac{f\pi}{2\bar{e}}$ . Furthermore, we have

$$\cos \frac{\bar{v}\pi}{2\bar{e}} = \cos \frac{\Omega_m + \pi - \alpha}{2} = \frac{\mu \sin \frac{\alpha}{2}}{\sqrt{\mu^2 + \cos^2 \frac{\alpha}{2}}}.$$

From this, it follows that

$$\mu = \frac{\cos \frac{\bar{v}\pi}{2\bar{e}} \cos \frac{\bar{f}\pi}{2\bar{e}}}{\sqrt{\sin^2 \frac{\bar{f}\pi}{2\bar{e}} - \cos^2 \frac{\bar{v}\pi}{2\bar{e}}}}.$$

Note that  $\sin \frac{\bar{f}\pi}{2\bar{e}} = \cos \left( \frac{\pi}{2} - \frac{\bar{f}\pi}{2\bar{e}} \right) = \cos \frac{(\bar{v}-2)\pi}{2\bar{e}}$ , and thus,

$$\mu = \frac{\cos \frac{\bar{v}\pi}{2\bar{e}} \cos \frac{\bar{f}\pi}{2\bar{e}}}{\sqrt{\cos^2 \frac{(\bar{v}-2)\pi}{2\bar{e}} - \cos^2 \frac{\bar{v}\pi}{2\bar{e}}}},$$

which implies, in particular, that the expression behind the square root is positive. Now, algebraic transformations yield

$$\sqrt{\mu^2 + \cos^2 \frac{\pi\bar{f}}{2\bar{e}}} = \frac{\cos \frac{\bar{v}\pi}{2\bar{e}} \cos \frac{(\bar{v}-2)\pi}{2\bar{e}}}{\sqrt{\cos^2 \frac{(\bar{v}-2)\pi}{2\bar{e}} - \cos^2 \frac{\bar{v}\pi}{2\bar{e}}}}.$$

Thus,

$$\Omega_a = \frac{\bar{v}\pi}{2\bar{e}} + \arccos \frac{\sqrt{\cos^2 \frac{(\bar{v}-2)\pi}{2\bar{e}} - \cos^2 \frac{\bar{v}\pi}{2\bar{e}}}}{\cos \frac{(\bar{v}-2)\pi}{2\bar{e}}} - \frac{\pi}{2} = \frac{\bar{v}\pi}{2\bar{e}} + \arcsin \frac{\cos \frac{\bar{v}\pi}{2\bar{e}}}{\cos \frac{(\bar{v}-2)\pi}{2\bar{e}}} - \frac{\pi}{2}.$$

Combining this with (12) yields

$$\hat{n} = \frac{2\pi\bar{v}}{2\bar{e} \arcsin \frac{\cos \frac{\bar{v}\pi}{2\bar{e}}}{\cos \frac{(\bar{v}-2)\pi}{2\bar{e}}} - (\bar{e} - \bar{v})\pi}. \quad (13)$$

Now, the formula in Theorem 1 is an immediate consequence of (13) and the identity  $\bar{e} = \bar{v} + \bar{f} - 2$ .  $\square$

Before stating a supplement of Theorem 1, recall that by a result of Steinitz (1906, 1922), there is a convex polyhedron with  $v$  vertices and  $f$  faces if and only if  $v \geq 4$ , and  $\frac{1}{2}v + 2 \leq f \leq 2v - 4$ , or equivalently,  $4 + \frac{1}{2}(v - 4) \leq f \leq 4 + 2(v - 4)$ .

**Proposition 1** Define the function

$$\hat{n}(t, \bar{v}) = \frac{2\pi\bar{v}}{2(\bar{v} + \bar{f} - 2) \arcsin\left(\frac{\cos\left(\frac{\bar{v}\pi}{2(\bar{v}+\bar{f}-2)}\right)}{\cos\left(\frac{(\bar{v}-2)\pi}{2(\bar{v}+\bar{f}-2)}\right)}\right) - (\bar{f} - 2)\pi}$$

as in Theorem 1, where  $\bar{v} > 4$ , and  $\bar{f} = 4 + t(\bar{v} - 4)$  for some  $\frac{1}{2} \leq t \leq 2$ . Then  $\hat{n}(t, \bar{v})$  is a strictly decreasing function of  $t$  for all values  $\bar{v} > 4$ .

**Proof** Let  $\bar{e} = \bar{v} + 4 + t(\bar{v} - 4) - 2 = (t + 1)\bar{v} + 2 - 4\bar{v}$ , and observe that the conditions in Proposition 1 for  $\bar{v}$  and  $t$  are equivalent to  $\frac{3}{2}\bar{v} \leq \bar{e} \leq 3\bar{v} - 6$ .

An elementary computation yields that

$$\frac{\partial \hat{n}(t, \bar{v})}{\partial t} = \frac{2\pi\bar{v}(\bar{v} - 4)F}{G},$$

where

$$G = \bar{e} \left( 2\bar{e} \arcsin \frac{\cos \frac{\bar{v}\pi}{2\bar{e}}}{\cos \frac{(\bar{v}-2)\pi}{2\bar{e}}} + (\bar{v} - \bar{e})\pi \right)^2 \cos \frac{(\bar{v} - 2)\pi}{2\bar{e}} \sqrt{\cos^2 \frac{(\bar{v} - 2)\pi}{2\bar{e}} - \cos \frac{\bar{v}\pi}{2\bar{e}}},$$

and

$$F = \bar{e} \left( \pi - 2 \arcsin \frac{\cos \frac{\bar{v}\pi}{2\bar{e}}}{\cos \frac{(\bar{v}-2)\pi}{2\bar{e}}} \right) \cos \frac{(\bar{v} - 2)\pi}{2\bar{e}} \sqrt{\cos^2 \frac{(\bar{v} - 2)\pi}{2\bar{e}} - \cos \frac{\bar{v}\pi}{2\bar{e}}} - (\bar{v} - 2)\pi \sin \frac{\pi}{\bar{e}} - 2\pi \sin \frac{(\bar{v} - 1)\pi}{2\bar{e}}$$

Note that under our conditions, the above partial derivative of  $\hat{n}$  is negative if  $F$  is negative on the domain  $\bar{v} > 4$ ,  $\frac{3}{2}\bar{v} \leq \bar{e} \leq 3\bar{v} - 6$ .

Using algebraic transformations, we obtain that

$$F = 2\bar{e} \left( \left( \frac{\pi}{2} - \arcsin \frac{\cos x}{\cos y} \right) \cos y \sqrt{\cos^2 y - \cos^2 x} - y \sin(x - y) - (x - y) \sin(x + y) \right), \quad (14)$$

where  $x = \frac{\bar{v}\pi}{2\bar{e}}$  and  $y = \frac{(\bar{v}-2)\pi}{2\bar{e}}$ . Here, the inequalities  $\bar{v} > 4$  and  $\frac{3}{2}\bar{v} \leq \bar{e} \leq 3\bar{v} - 6$  are equivalent to the inequalities  $\frac{\pi}{6} \leq x \leq \frac{\pi}{3}$  and  $\frac{\pi}{6} \leq y < x$ . Thus, we prove that the

expression on the right-hand side of (14) is negative on this domain. Simplifying this expression, we have

$$F = 2\bar{e} \sin(x - y)((A - B) \sin(x + y) - y), \quad (15)$$

where

$$A = \frac{\frac{\pi}{2} - \arcsin \frac{\cos x}{\cos y}}{\sqrt{1 - \frac{\cos^2 x}{\cos^2 y}}} = \frac{\arcsin \sqrt{1 - \frac{\cos^2 x}{\cos^2 y}}}{\sqrt{1 - \frac{\cos^2 x}{\cos^2 y}}}, \quad B = \frac{x - y}{\sin(x - y)}.$$

To estimate the values of  $A$  and  $B$ , we use the fact that the function  $z \mapsto \frac{z}{\sin z}$  is strictly increasing on the interval  $0 < z < \frac{\pi}{2}$ . Our inequalities imply that  $0 < x - y < \frac{\pi}{6}$ ,  $0 < \arcsin \sqrt{1 - \frac{\cos^2 x}{\cos^2 y}} < \arcsin \sqrt{\frac{2}{3}}$ , and  $x \leq 2y$ . From the first two inequalities it follows that  $A - B \leq 0.123$ . Substituting this and the third inequality into (15), we obtain

$$F < 2\bar{e} \sin(x - y)y \left( 0.369 \frac{\sin(3y)}{3y} - 1 \right) < 0,$$

proving Proposition 1.  $\square$

**Remark 5** Note that by Proposition 1, for any value  $\bar{v} \geq 4$ ,  $\hat{n}(t, \bar{v})$  attains all values between  $\hat{n}\left(\frac{1}{2}, \bar{v}\right)$  and  $\hat{n}(2, \bar{v})$ .

## 2.2 Proof of Theorem 2: Explicit Computation of Errors

**Proof** Table 2 proves Theorem 2.  $\square$

## 3 Summary

In this paper we took a close look at Plato's atomistic model which proposed the five regular solids as the building blocks of the Universe. On one hand, we found that this approach contains some quantitative errors, as four of the five Platonic solids do not fill space without gaps. This mismatch led to criticism of Plato's ideas, most notably by Aristotle.

However, not only did our computations show that the quantitative errors in Plato's model are quite small, we also introduced another, holistic interpretation of the Platonic approach (possibly closer to Plato's original ideas) which we interpreted as a *mean field approximation* to some special convex mosaics. We developed this idea a little further to obtain a formula which serves as a mean field approximation to *all*

*convex mosaics in  $d = 3$  dimensions.* This mean field theory not only offers a good quantitative approximation to a large variety of known mosaics, it may also help to explain some curious facts associated with 3D mosaics. We represented mosaics on the  $[\bar{n}, \bar{v}]$  symbolic plane of average nodal and cell degrees. While 2D mosaics appear on a curve [given by formula (2)], however, the 60 three-dimensional mosaics examined in this paper appear *scattered in the vicinity* of an (imaginary) curve. Since our mean field theory is a straightforward generalization of Plato's original approach, we called the resulting geometric constructions Platonic mosaics. If interpreted over the admissible domain of pairs  $(f, v)$ , Platonic mosaics provide a reasonable approximation of that imaginary curve showing that this theory, despite its simplicity, captures some essential geometric features of 3D mosaics.

Whether or not Platonic mosaics contribute to the vindication of Plato's original views about the Universe is certainly not a mathematical question. Nevertheless, we hope that these geometric constructions may help to reveal some of the secrets which inspired Plato: the geometric patterns in which convex polyhedra may or may not fill space without gaps.

**Acknowledgements** Open access funding provided by Budapest University of Technology and Economics (BME). The authors sincerely thank Liliana Albertazzi for drawing their attention to some of the most interesting philosophical aspects of this problem. This research was supported by the NKFIH Hungarian Research Fund Grant 119245 and of Grant BME FIKP-VÍZ by EMMI is kindly acknowledged. ZL has been supported by Grant UNKP-18-4 New National Excellence Program of EMMI and the János Bolyai Research Scholarship of the Hungarian Academy of Sciences.

**Open Access** This article is distributed under the terms of the Creative Commons Attribution 4.0 International License (<http://creativecommons.org/licenses/by/4.0/>), which permits unrestricted use, distribution, and reproduction in any medium, provided you give appropriate credit to the original author(s) and the source, provide a link to the Creative Commons license, and indicate if changes were made.

## References

- Albertazzi L (ed) (2013) Handbook of experimental Phenomenology. Wiley, New York
- Atiyah M, Sutcliffe P (2003) Polyhedra in physics, chemistry and geometry. Milan J Math 71(1):33–58
- Ball P (2004) The elements: a very short introduction. Oxford University Press, Oxford
- Chung PN, Fernandez MA, Li Y, Mara M, Morgan F, Plata IR, Shah N, Vieira LS, Wikner E (2012) Isoperimetric pentagonal tilings. Not Am Math Soc 59:632–640
- Coxeter HSM (1956) Regular honeycombs in hyperbolic space. Proceedings of the international congress of mathematicians, 1954, Amsterdam. 3:155–169
- Deza M, Shtogrin M (2000) Uniform partitions of 3-space, their relatives and embedding. Eur J Combin 21:807–814. <https://doi.org/10.1006/eujc.1999.0385>
- Domokos G, Lángi Z (2019) On some average properties of convex mosaics. Arxiv preprint <https://arxiv.org/pdf/1905.00721>
- Exhibit AN1927.2727-31 Neolithic Carved Sandstone Balls. Ashmolean Museum, University of Oxford
- Grünbaum B (1994) Uniform tilings of 3-space. Geombinatorics 4:49–56
- Heath TL (1921) A history of Greek mathematics, vol 2. Clarendon Press, Oxford
- Johnson NW (1991) Uniform polytopes (manuscript)
- Lloyd GER (1968) Aristotle: the growth and structure of his thought. Cambridge University Press, Cambridge, pp 166–169. ISBN 978-0-521-09456-6
- Macauley D (2010) Elemental philosophy: earth, air, fire, and water as environmental ideas. State University of New York Press, Albany
- Perl ED (1998) The demiurge and the forms: a return to the ancient interpretation of Plato's timaeus. Anc Philos 18:81–92



- Plato (2015) *Timaeus*. Translated by B. Jowett. Aeterna Press (original edition: MacMillan and Co. London, 1892)
- Schneider R, Weil W (2008) *Stochastic and integral geometry*. Springer, Berlin
- Schulte E (1993) Tilings, handbook of convex geometry, vol A, B. North-Holland, Amsterdam, pp 899–932
- Senechal M (1981) Which tetrahedra fill space? *Math Mag* 54(5):227–243
- Steinitz E (1906) Über die Eulersche Polyederrelationen. *Arch Math Phys* 11:86–88
- Steinitz E (1922) Polyeder und Raumeinteilungen. *Enzykl Math Wiss* 3(Geometrie), Part 3AB12:1–139
- Whitehead AN (1938) *Forms of process lecture five in modes of thought*. Macmillan, New York, pp 117–142
- Wilberding J, Horn C (2012) *Neoplatonism and the philosophy of nature*. Oxford University Press, Oxford. <https://doi.org/10.1093/acprof:oso/9780199693719.001.0001>
- Wilczek F (2011) Beautiful Losers NOVA magazine (PBS) December 30th. <https://www.pbs.org/wgbh/nova/article/beautiful-losers/>
- Zeyl D, Sattler B (2019) Plato's *Timaeus*. In: Edward NZ (ed) *The Stanford Encyclopedia of Philosophy* (Summer 2019 Edition). <https://plato.stanford.edu/archives/sum2019/entries/plato-timaeus/>

**Publisher's Note** Springer Nature remains neutral with regard to jurisdictional claims in published maps and institutional affiliations.